An Acad Bras Cienc (2024) 96(2): e20230375 DOI 10.1590/0001-3765202420230375
Anais da Academia Brasileira de Ciências | *Annals of the Brazilian Academy of Sciences*
Printed ISSN 0001-3765 I Online ISSN 1678-2690
www.scielo.br/aabc | www.fb.com/aabcjournal

CHEMICAL SCIENCES

Design, synthesis and identification of novel molecular hybrids based on naphthoquinone aromatic hydrazides as potential trypanocide and leishmanicidal agents

ROSANE D. CEZAR, ADRIANO O. DA SILVA, ROSÂNGELA S. LOPES, CELSO V. NAKAMURA, JEAN HENRIQUE S. RODRIGUES, ESTELA MARIANA G. LOURENÇO, SUMBAL SABA, ADILSON BEATRIZ, JAMAL RAFIQUE & DÊNIS P. DE LIMA

Abstract: In pursuit of potential agents to treat Chagas disease and leishmaniasis, we report the design, synthesis, and identification novel naphthoquinone hydrazide-based molecular hybrids. The compounds were subjected to *in vitro* trypanocide and leishmanicidal activities. *N*'-(1,4-Dioxo-1,4-dihydronaphthalen-2-yl)-3,5-dimethoxybenzohydrazide (**13**) showed the best performance against *Trypanosoma cruzi* (IC_{50} 1.83 μM) and *Leishmania amazonensis* (IC_{50} 9.65 μM). 4-Bromo-*N*'-(1,4-dioxo-1,4-dihydronaphthalen-2-yl)benzohydrazide (**16**) exhibited leishmanicidal activity (IC_{50} 12.16 μM). Regarding trypanocide activity, compound **13** was low cytotoxic to LLC-MK2 cells (SI = 95.28). Furthermore, through molecular modeling studies, the cysteine proteases cruzain, rhodesain and CPB2.8 were identified as the potential biological targets.

Key words: Neglected diseases, Trypanocide activity, Leishmanicidal activity, Lawsone, Naphthoquinone hydrazide hybrids.

INTRODUCTION

Neglected diseases (NTD) are a distinct group of transmissible diseases that occur in tropical and subtropical regions of the world. They are especially common in low-incoming populations that affect more than a billion people and cost emerging economies billions of dollars every year (Warusavithana et al. 2022, WHO 2020).

Leishmaniasis and Chagas disease, caused by the kinetoplastid parasites *Leishmania* spp and *Trypanosoma cruzi*, respectively, are public health problems in countries where these diseases are prevalent. They are considered to be within the most relevant group of neglected tropical diseases (Nicolás-Hernández et al. 2023, Silva-Jardim et al. 2014).

Chagas disease occurs in 21 countries in Latin America and is estimated that 8 million people are infected worldwide (Vásconez-González et al. 2023). *T. cruzi* enters the human bloodstream mainly through wounded skin or mucous membranes with infected faeces from triatomine insects. This infection in humans is characterized by three distinct clinical phases as following: 1) acute, which causes fever and edema at infection point (chagoma), 2) generally asymptomatic intermediate phase and, 3) chronic phase. Almost 30% of infected patients develop the chronic phase, which may lead to clinical manifestations such as cardiac, gastrointestinal, and cardiodigestive forms of Chagas disease (Abras et al. 2022). More than 50% of patients who enter the chronic form die within 7 months

to 2 years of the initial symptoms (Abras et al. 2022, Nasim & Qureshi 2023, Salas et al. 2008, Silva-Jardim et al. 2014, WHO 2017).

Leishmaniasis, caused by protozoan parasites of the genus *Leishmania*, is a vector-borne infection that can occur in tropical and subtropical regions of the world. Depending on the region, the disease is spread by different species of insects of the genus Phlebotomus or Lutzomyia (Venkatesan et al. 2023). Clinical expressions depend on the *Leishmania* species. Visceral forms of leishmaniasis are responsible for most deaths and the most common manifestation are skin lesions (de Castro et al. 2013, Olivier et al. 2005, Singh et al. 2023).

Sadly, currently there are no vaccines available to prevent these infections. The main option to treat these diseases is chemotherapy using pentavalent antimonials, amphotericin B, miltefosine, paromomycin, and pentamidine. However, these medications are associated with various adverse effects (Herwaldt 1999, Silva-Jardim et al. 2014, Verdan et al. 2023). Therefore, there is a high demand for new efficient and safer drug scaffolds to treat Chagas disease and leishmaniasis (Jorge et al. 2023, Rycker et al. 2023).

Among the potential medicinal chemistry tools that can circumvent this issue, there is the molecular hybridization strategy for drug discovery. This approach is based on the design of new chemical entities by the fusion of bioactive molecular fragments derived from known bioactive molecules (Burkner et al. 2023, Pedroso et al. 2023, Lourenço et al. 2023, Wang et al. 2023). Usually, it is essential to verify the synergistic characteristics of the two fragments in order to plan the new target molecular entity (Dong et al. 2023, Fershtat & Makhova 2017, Fraga 2009, Langdon et al. 2010, Lazar et al. 2004, Wang et al. 2023, Viegas-Junior et al. 2007).

Hence, examining molecular frameworks to design novel antiparasitic agents preferably endowed with multitarget features, the 1,4-naphthoquinone skeletons emerged as promising starting material candidates for developing new bioactive hybrid agents (Navarro-Tovar et al. 2023). The reason for this is that the literature describes, for example, lawsone, α-lapachone, β-lapachone (Figure 1) and their congeners as having diverse biological properties, including trypanocide and leishmanicidal activities (Cardoso et al. 2017, Dantas et al. 2017, da Silva et al. 2013, Guimarães et al. 2013, Rani et al. 2022, Naujorks et al. 2015).

Consequently, hydrazide-bearing molecules and similar scaffolds such as *N*'-(1, 4-naphtho-quinone-2-yl) isonicotinohydrazide (I), benzohydrazones (II), and quinoline-piperazine propionic acid hydrazones (III) are also reported as important compounds endowed with trypanocide, antibacterial, antiamoebic, antimalarial, anticancer, antiviral, anti-inflammatory, antiatherosclerotic and antifungal activities (Bouhadir et al. 2017, Caffrey et al. 2002, Hu et al. 2023, Kavitha et al. 2015, Kumar et al. 2017, Reddy et al. 2013)

Considering molecular hybridization strategy, we have come across only two reports in the literature in which lawsone (Figure 1) was subjected to a reaction with aromatic hydrazide to form C-2 substituted bioactive naphthoquinones (Dudley et al. 1969, Hu et al. 2023, Kavitha et al. 2015). As part of our research interest in synthesis and biological evaluation of heterocyclic compounds (Botteselle et al. 2021, dos Santos et al. 2021, 2022, Franco et al. 2021, Moraes et al. 2023, Rafique et al. 2020, Scheide et al. 2020, Veloso et al. 2021, Vitor et al. 2021), we decided to prepare naphthoquinone aromatic hydrazide-based molecular hybrids, using a simple, inexpensive and reliable protocol. These new frameworks of *N*'-(1,4-naphtho-quinone-2yl)

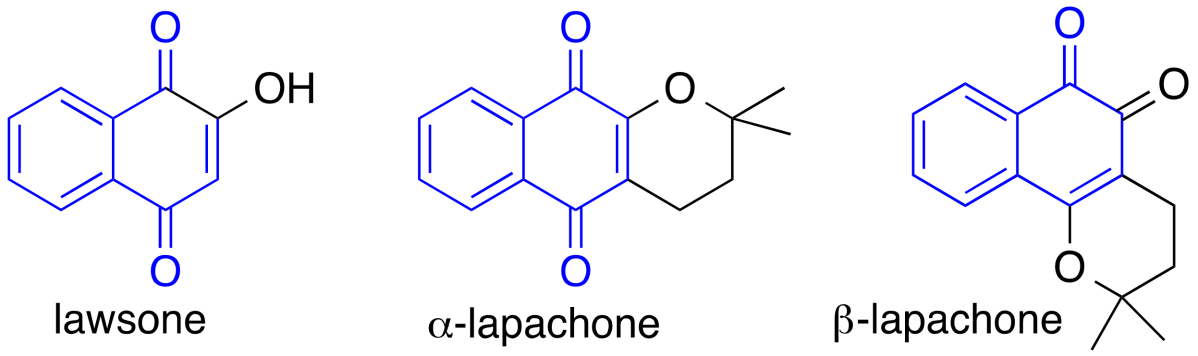

Figure 1. Molecular structure of lawsone and analogous.

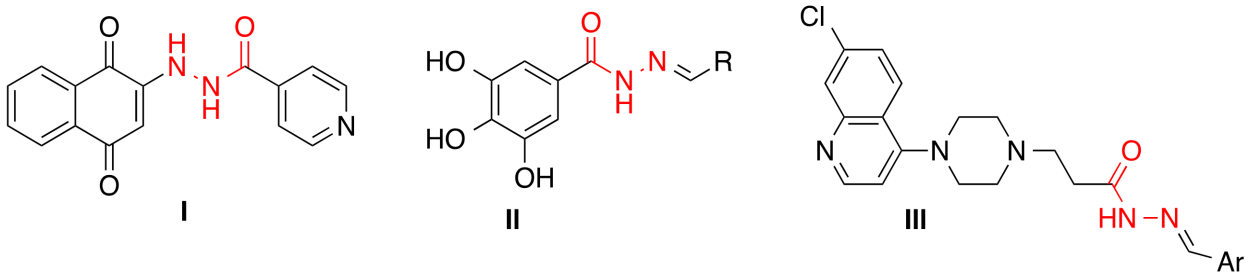

Figure 2. Hydrazine linker in bioactive molecules.

hydrazide (Figure 3) were tested as potential trypanocide and leishmanicidal drug prototypes.

RESULTS AND DISCUSSION

Figure 4 shows the synthetic route designed to achieve the fused molecules of naphthoquinone hydrazides. Initially, we selected substituted benzoic acid starting materials (**1**-**4**) that were subjected to simple esterification reactions with methanol under acid catalysis. The respective esters formed (**5**-**8**) were necessary to generate the aromatic hydrazides (**9-12**) of the aimed parent by treatment with hydrazine hydrate (Rodrigues et al. 2016). The key coupling step was then followed by the reaction of lawsone (Figure 1) with hydrazides (da Silva et al. 2013) to give the four corresponding target hybrids (**13**-**16**).

All compounds were characterized using high-resolution mass spectrometry (HRMS), Fourier transform infrared (FTIR) and, ^{13}C and ^{1}H nuclear magnetic resonance (NMR) spectroscopies. The compound **13**, for example, analyzed as $C_{19}H_{17}N_2O_5$ $[M+H]^+$, showed a molecular ion peak at *m/z* 353.1059 in its high-resolution mass spectrum. The relevant features of its ^{1}H NMR spectrum comprised the presence of two singlets at δ 9.49 and 10.71 corresponding to hydrogens bonded to the azide group. Furthermore, two doublets were recorded at δ 7.94 and δ 8.02, two multiplets at

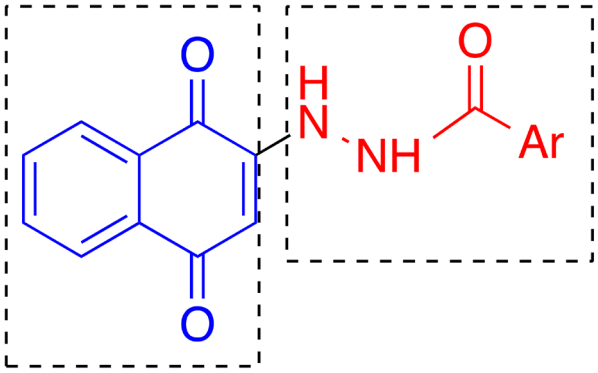

Figure 3. Targeted naphthoquinone aromatic hydrazide-based molecular hybrids.

δ 7.77 and δ 7.85, as well as a singlet at δ 5.67 due to the aromatic and olefinic protons of the naphthoquinone ring. A doublet at δ 7.08 and a singlet at δ 6.72 were attributed to the aromatic ring of the hydrazide moiety. Hydrogens of methoxy groups showed signals at δ 3.80. The appearance of absorptions at δ 182.6, δ 181.4 and δ 168.3 corresponding to three carbonyls along with the presence of methylene carbons at δ 102.1 and δ 148.9 as confirmed by ^{13}C (DEPT) spectra additionally corroborated the assigned structure.

The synthesized naphthoquinone hydrazide hybrids were evaluated for their *in vitro* activities against epimastigote forms *T. cruzi* and promastigote *L. amazonensis* and the results are registered in Table **I.**

Although scaffolds **14**-**16** were inactive against the epimastigote *T. cruzi*, this result is not considered insignificant when comparing these activities with the parent lawsone (IC_{50} 410 μM) (Muñoz et al. 2006). On the other hand, compound **13** (IC_{50} 1.83 μM) revealed a higher trypanocide activity than the reference drug benznidazole (IC_{50} 8.80 μM). An analysis of the structure-activity relationship (SAR) of the synthesized hybrids disclosed the dependence of trypanocide activity on the nature and pattern of substitution at the aromatic ring of the azide segment. Interestingly, comparing the 3,5-dimethoxy substitute compound (**13**) with the 3,4,5-trimethoxy substitute compound (**14**) (Table **I**), the latter significantly decreased its activity, suggesting a possible requirement to locate the molecules during interaction with biological receptors. Studies have stated that electronic and structural properties are important factors in the interaction between trypanocide quinone derivatives and biological receptors (Molfetta et al. 2005).

The results of *in vitro* antiproliferative assays in promastigote *L. amazonensis* showed that compounds **14** and **15** (IC_{50} >100) were inactive (Table **I**). However, compounds **13** (IC_{50} 9.65 μM) and **16** (IC_{50} 12.16 μM) displayed moderate leishmanicidal activity. According to

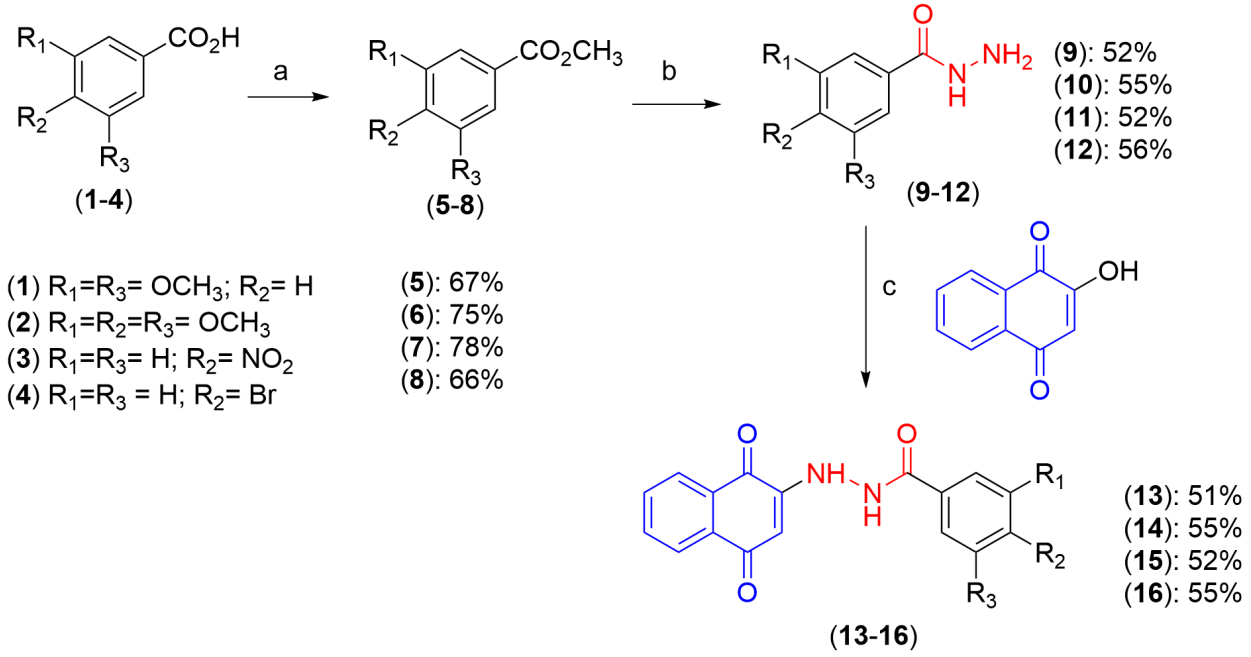

Figure 4. Synthetic route to prepare hybrids 13-16.

Muñoz and coworkers (31), the enhancement of the trypanocide and leishmanicidal activities of derivatives related to hydrazides, such as various disubstituted aromatic hydrazones, depends on the groups attached to each side of the molecules. Furthermore, the authors mentioned that molecules designed to be used as antiparasitic can be simultaneously active against *Trypanosoma* and *Leishmania,* since the parasites share proteins with very similar active site (Muñoz et al. 2006).

Biopharmaceutical aspects are also crucial to be measured in drug candidates. In particular, logP values are vastly discussed in medicinal chemistry since the postulation of the rule of five. This parameter analysis the solubility profile of a compound in an immiscible biphasic system of lipids and water (Bhal 2007, Brown 2012). Considering the physiological environment, this aspect is of great importance, as it can provide information on whether a compound will penetrate the cell membrane or be easily solubilized in an aqueous medium such as blood. In the study of rule of five, Lipinski et al. (1997) investigated the biopharmaceutical aspects of a set of standard drugs. Between them, a result of clogP ≤ 5 was postulated as being necessary for an ideal prototype. Meanwhile, logS are directly related with the solubility in water of a molecule and values close to −4 were defined as standard for a drug candidate (Sander 2001). All tested compounds had logS values close to −4 and logP ≤ 5, following the postulated characteristics (Table I). It is also important to highlight that Benznidazole presented a logS value considerably greater than -4, which represents a violation of what is postulated for biopharmaceutical aspects of a drug. Therefore, compound **13** is not only more active than Benznidazole for the epimastigote form of *T. cruzi*, but it is also more viable considering its potential for greater bioavailability.

Cytotoxicity of all hybrids (**13**-**16**) was determined using the MTT LLC-MK2 cell assay (Rodrigues et al. 2014) to determine whether the observed activities are due to their trypanocide and leishmanicidal efficacy or cytotoxicity (Table **II**).

As is evident, compound **13** was not cytotoxic for LLC-MK2 cells (SI = 95.28) with respect to trypanocide activity and, although this index was lower for leishmanicidal activity (SI = 18.06), it is still attractive if we take into account the possibility of generating new derivatives with some skeletal modification. For compound **16**, it was nearly twice as cytotoxic against *Leishmania*

Table I. LogP, logS, trypanocidal and leishmanicidal activities of compounds tested against epimastigote *T. cruzi* and promastigote *L. amazonensis* forms.

Compound	logP[a]	logS[b]	[c]IC_{50} (μM) ± SD *T. cruzi*	[c]IC_{50} (μM) ± SD *L. amazonensis*
13	2.02	-4.11	**1.83 ± 0.36**	**9.65 ± 0.36**
14	2.14	-4.13	114.10 ± 9.12	>100
15	1.50	-4.03	117.63 ± 10.96	>100
16	2.69	-4.88	86.89 ± 7.00	**12.16 ± 0.92**
Benznidazole[d]	0.49	-2.06	8.80 ± 0.4	-
Amphotericin B[d]	-0.39	-5.37	-	0.065

Values represent the mean ± S.D. of duplicate determination. [a]LogP, octanol/water partition coefficient measured by SwissADME (Daina et al. 2017); [b]LogS expressed as log (g/100 g water) measured by SwissADME (Daina et al. 2017); [c] IC_{50} is the concentration of the compound that is required for 50% inhibition *in vitro*. [d] Positive controls.

versus LLC-MK2 cells (SI = 19.52) (Table II) and appears to have potential for the development of new bioactive halogen analogues.

For drug development, target identification is crucial to follow-up studies, aiding medicinal chemistry efforts (Schenone et al. 2013). In the context of neglected diseases such as Leishmaniasis and Chagas disease, the target-based strategy has been the dominant tool over the last decades due to the advances in molecular biology and urgency to discover new effective drugs (Lourenço et al. 2023, Gilbert 2013). Therefore, to deeply analyze the influence of different substituents of tested compounds on the antiparasitic action, it is necessary to identify their potential pharmacological targets. Although the results of antiparasitic activity for this set of compounds are unprecedented, previous studies in the literature may shed light on the investigation of potential biological targets behind their pharmacological effects.

A previous study investigated the ability to inhibit the cysteine proteases cruzaine and rhodesain by a set of compounds based on 1,4-naphthoquinone core (Silva et al. 2021). Interestingly, CR-70 was active against these proteases and had a very similar structure to those tested in our study. (Figure 5). Considering that structurally similar molecules commonly have similar biological activities (Martin et al. 2002), we performed docking and molecular dynamics simulations using cruzain and rhodesain as proteins. In addition, to select the ligands used in molecular modeling studies, we used the Activity cliff theory as a tool. Activity cliffs (ACs) are of particular interest in structure-activity relationship (SAR) analysis and compounds optimization. ACs are defined as pairs or groups of molecules marked by their high structural similarity but large difference in potency (Stumpfe et al. 2019). Between the tested compounds, **13** and **15** can be considered as an AC for both antileishmanial and anti-*T. cruzi* activities. Therefore, these compounds were selected to better understanding a potential SAR for this set of antiparasitic molecules.

The differences in the potency of compounds **13** and **15** were confirmed by the distinct binding mode positions at cruzain active site. Compound **15** only occupied one hydrophobic pocket of the protein biding site (Figure 6a). As a result, this compound mainly made hydrophobic interactions with the amino acid residues (Figure 6b). However, the replacement of a nitro by a methoxy group, as well as the addition of a second methoxy group in R1 resulted in a greater interaction with the amino acid residues of the active site. Between them, the hydrogen bond, considered as a strong interaction, with Asp161 stood out (Figure 6c). Furthermore, **13** occupied the entire active site of cruzain (Figure 6d), explaining its high antiparasitic activity demonstrated by *in vitro* assays.

Table II. **Cytotoxicity of naphthoquinone hydrazide hybrids on LLC-MK2 cells and their selectivity index (SI).**

Compound	LLC-MK2 CC_{50} (μM) ± SD	SI *T. cruzi* (epimastigote)	SI *L. amazonensis* (promastigote)
13	174.37 ± 18.52	95.28	18.06
14	269.08 ± 44.05	2.35	> 2.69
15	152.29 ± 18.95	1.29	> 1.52
16	237.36 ± 29.62	2.73	19.52

CC_{50} = concentration of the compound that causes death in 50% of viable cells in the culture medium after 96 h of exposition. IC_{50} = minimum inhibition concentration to inhibit 50% of the protozoa in its culture medium. SI = CC_{50} LLC-MK2 / IC_{50} of epimastigote or promastigote forms.

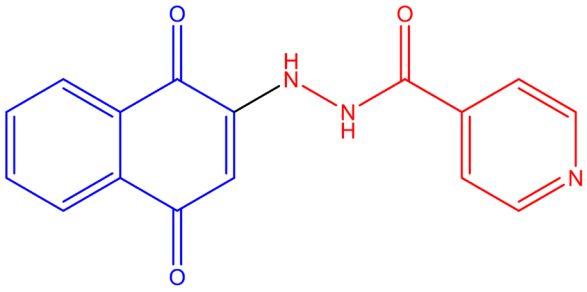

Figure 5. Chemical structure of compound CR-70.

The same molecular scenario was identified considering the interactions of the tested compounds with rhodesain. Although the binding modes of **15** and **13** were similar (Figures 7a and 7c), the types of intermolecular interactions with the protein's amino acid residues were notably different. Likewise, hydrophobic interactions were the only ones made between compound **15** and the rhodesain binding site. (Figures 7b). In contrast, compound **13** demonstrated hydrophobic interactions as well as a hydrogen bond with Gln19 (Figure 7d). Combined, these results reinforce the better *in vitro* results of compound **13** and explain the potency differences between this AC.

Cruzain and rhodesain are cysteine proteases widely expressed in *T. cruzi*. However, the compounds have also been tested and proven to be active against promastigotes forms of *L. amazonensis*. This fact may be related to the expression of other cysteine proteases by *Leishmania* parasite such as CPB which are structurally very similar to cruzain and rhodesain. It is important to highlight that both mentioned proteins are L-type cathepsins, resulting in similar inhibition capacity by the prototypes (Lourenço et al. 2023, Rebello et al. 2010). CPB is a virulence factor and plays an important role for parasite survival in mammalian host cells. Although it is more expressed in amastigotes, some previous works

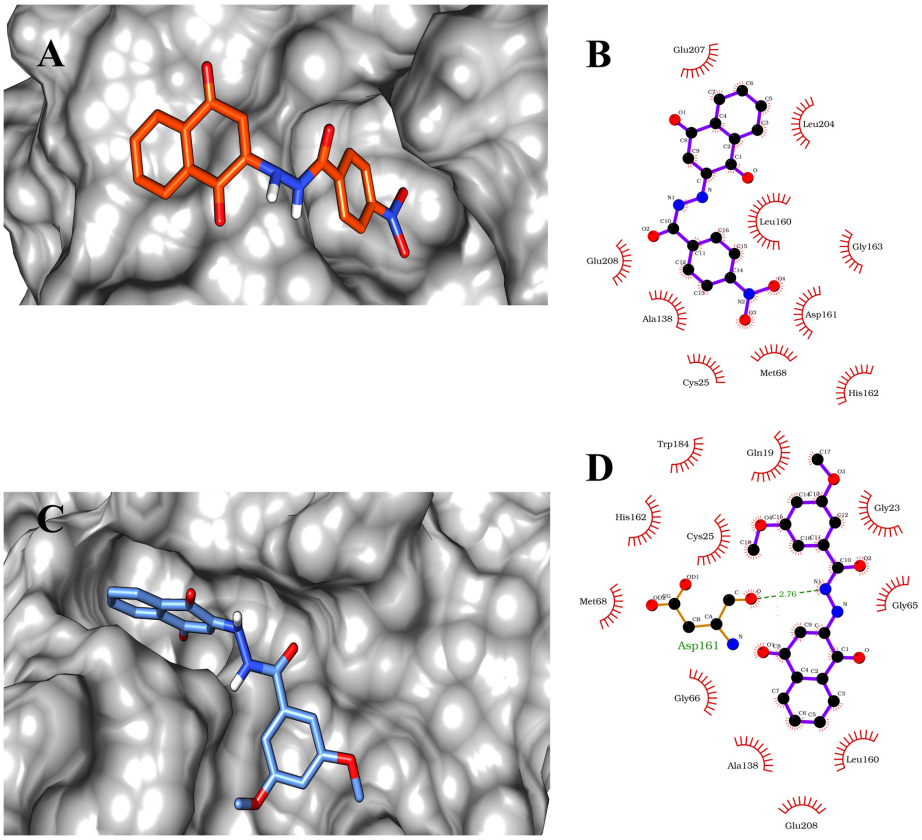

Figure 6. Binding mode positions of compounds 15 (a) and 13 (c), and 2D representations of these compounds (b and d) at the biding site of cruzain (PBD ID: 1AIM).

have demonstrated the presence of CPB on the surface of the promastigote form. Therefore, this cysteine protease could be a potential target for molecular hybrids based on naphthoquinone aromatic hydrazide.

Analyzing the output results of compounds **13** and **15**, a difference in type of molecular interactions with amino acids residues was again observed. Both compounds had occupied all the pockets of the active site of CPB2.8 (Figures 8a and 8c). However, compound **13** showed two hydrogen bonds with Gly191 and Gln144 as well as hydrophobic interactions (Figure 8d). Meanwhile, compound **15** made only hydrophobic interactions with the amino acid residues (Figure 8b).

The calculated binding free energy values reflected the strongest intermolecular interactions made by compound **13** on cruzain, rhodesaine and CPB2.8. Between the results, the lowest binding-free energy was obtained by the interaction between **13** and the proteins cruzain and rhodesaine (-1.25 and -0.94 kcal·mol^{-1}, respectively). The results are 3.2 and 2.93-fold higher than those demonstrated for compound **15** (Table III). The most promising results for *T. cruzi* cysteine proteases also reinforce the *in vitro* results since compound **13** was more active against epimastigote forms. Furthermore, binding free energy values from simulations using CPB2.8 as the protein also demonstrate a more stable interaction with **13** by 2.27-fold (Table III). Combined, the molecular modelling approaches pointed out that cysteine proteases may be the potential targets for naphthoquinone aromatic hydrazide-based molecular hybrids and demonstrated the importance of a polar substituent on R1.

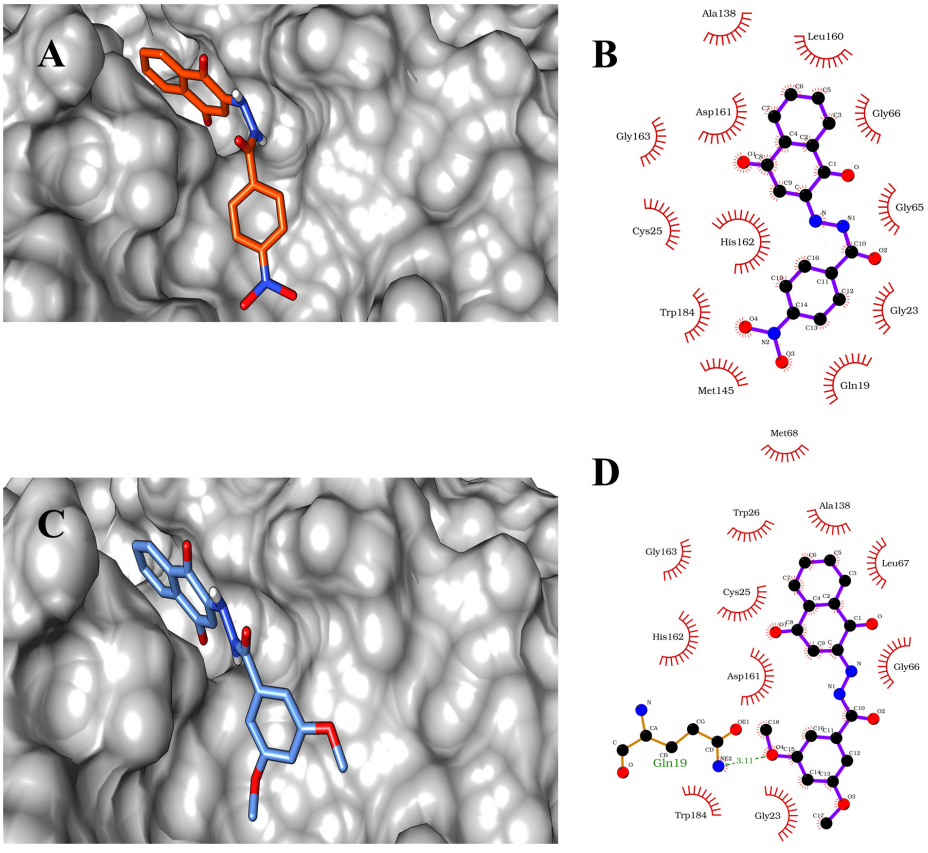

Figure 7. Binding mode positions of compounds 15 (a) and 13 (c), and 2D representations of this compounds (b and d) at the biding site of rhodesain (PBD ID: 6EXQ).

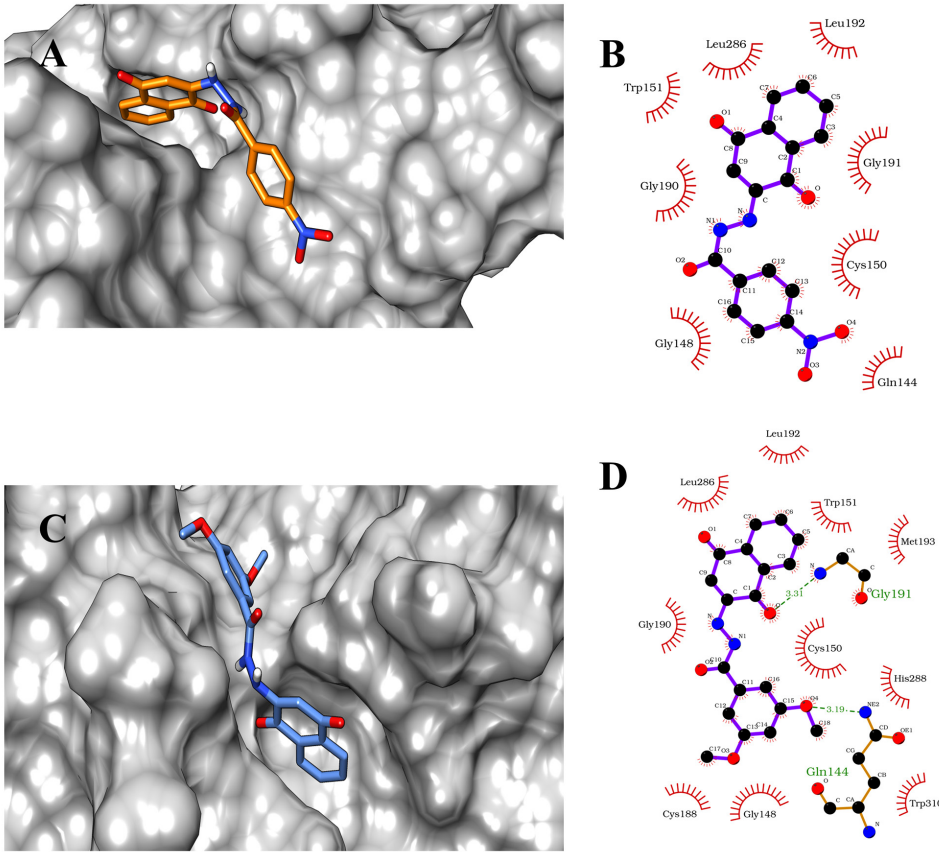

Figure 8. Binding mode positions of compounds **15** (a) and **13** (c), and 2D representations of this compounds (b and d) at the biding site of CPB2.8.

CONCLUSIONS

Based on the molecular hybridization strategy, we have designed, synthesized, and identified novel molecular hybrids based on naphthoquinone aromatic hydrazides (**13**-**16**). Among them, compound **13** showed antileishmanial activity and a higher trypanocidal activity than standard benznidazole, also being non-cytotoxic to LLC-MK2 cells. This representative scaffold suggested a dependence of electronic and structural molecular features during the interaction with the biological receptors *Trypanosoma* and *Leishmania*. Although compound **16** demonstrated lower leishmanicidal activity than standard, it could serve as a molecular basis for the planning of additional bioactive halogen derivatives. Through molecular modelling studies, cysteine proteases were pointed as a potential target behind the antiparasitic action and the importance of a polar substituent on R1 was confirmed, Consequently, we assume that our findings substantiate the potential of the present approach and will inspire complementary studies on the discovery of novel antiparasitic drug prototypes related to these molecular frameworks.

Table III. Calculated energy values for the interaction of 13 and 15 with cruzain, rhodesain and CPB2.8

Enzyme	Binding-free energy[a]
13	
Cruzain	-1.25
Rhodesaine	-0.94
CPB2.8	-0.68
15	
Cruzain	-0.39
Rhodesaine	-0.32
CPB2.8	-0.30

[a]**All energy values are expressed in kcal·mol^{-1}.**

EXPERIMENTAL SECTION

Chemistry

All reagents were analytical grade and were used without further purification. Chromatographic purification was performed on silica gel (Merck, 100-200 mesh) and analytical thin layer chromatography (TLC) was performed on silica gel 60-F_{254}. The ^{1H} NMR (300 MHz) and ^{13}C NMR (75 MHz) spectra were measured with a Bruker Avance DPXT-300 spectrometer with $CDCl_3$ and DMSO-d_6 as solvents and recorded in ppm relative to the internal tetramethylsilane standard (TMS). The ^{1}H NMR spectra are reported as follows: ppm (multiplicity, coupling constant J/Hz, number of protons). Multiplicity is abbreviated as follows: s (singlet), d (doublet), dd (doublet of doublets), t (triplet), m (multiplet), br (broad signal). The coupling constants (*J*) are quoted in Hertz and recorded to the nearest 0.1 Hz. High resolution mass spectrometry (HRMS) was performed on a UFLC Shimadzu LC-20AD apparatus, with and IES-Q-QTOF-microTOF III detector (Bruker Daltonics) in chemical ionisation positive ion mode (m/z 120-1200). Samples were prepared with 0.1 g/mL (methanol/ water 7:3) and injected 1μL, using elution gradient water (phase A) and acetonitrile (phase B), both with 1% acetic acid, 50% isocratic method and a running time of 3 min. The infrared spectra were recorded on a Bomen FT-IR-MB100FT-IR spectrometer and reported as wavenumbers (cm^{-1}).

General procedure for synthesis of esters (5-8)

Substituted carboxylic acids (**1-4**) (1.1 mmol) previously solubilized in dry methanol (30 mL) were added to a 50 ml round bottom flask, followed by dropwise addition of H_2SO_4 (1.3 mL). The reaction mixture was then stirred and heated under reflux for 4 h. After this period, the TLC analysis indicated the complete consumption of the starting material. The excess of solvent was removed by rotoevaporation, and the mixture was neutralized with sodium bicarbonate. The organic layer was extracted with ethyl acetate (3 x 20 mL), washed with water (3 x 25 mL) and, dried in $MgSO_4$. The drying agent was removed by filtration and the solvent was removed by rotoevaporation to give the product as a colorless oil.

General procedure for synthesis of hydrazides (9-12)

Substituted esters (**5**-**8**), resulting from acids (**1**-**4**), respectively, (1.3 mmol) along with hydrazine, were added to a 25 ml round bottom flask. The mixture was stirred at room temperature overnight. After this period, the reaction mixture was poured into a beaker containing chipped ice. The precipitated mixture was then subjected to simple filtration, washed with distilled cold water (30 mL) and left to dry at room temperature.

General procedure for the synthesis of derivatives of hydrazides of lawsone (13-16)

Acylhydrazides (**9-12**), resulting from esters (5-8), respectively, (1.1 mmol) and 1,4-hydroxy-naphthoquinone (1.1 mmol) were added to a 25 ml round bottom flask containing acetic acid 80% (20 mL). The reaction mixture was kept under stirring overnight and monitored by TLC analysis. After this period, the product was filtered, washed with hexane (50 mL) and, recrystallised in ethanol.

N'-(1,4-dioxo-1,4-dihydronaphthalen-2-yl)-3,5-dimethoxybenzohydrazide (***13***) (Supplementary Material - Figure S1)

This compound was obtained from hydrazide **9**. Yield 51%. Orange solid. m.p. = 187-195 $^{\circ C.}$ ^{1}H NMR (300 MHz, DMSO-d_6) δ 3.80 (s, 6H), 5.67 (s, 1H), 6.72 (s, 1H), 7.08 (d, *J* = 1.8 Hz, 2H), 7.77 (m, 1H), 7.85 (m, 1H), 7.94 (d, *J* = 7.0 Hz, 1H), 8.02 (d, *J* = 7.0 Hz, 1H), 9.49 (br, 1H), 10.71 (s, 1H). ^{13}C NMR (75 MHz, DMSO-d_6,) δ 55.9 ($2CH_3$), 102.2 (CH), 104.5 (CH), 105.8 (CH), 125.9 (CH), 126.3 (CH), 130.9 (C), 132.9 (C), 133.2 (C), 134.4 (CH), 135.5 (CH), 148.9 (C),

160.9 (C), 165.3 (C), 181.4 (C=0), 182.8 (C=O). FT-IR (KBr, cm^{-1}) v_{max} 3289-3412 (NH), 1666-1681 (C=O), 1457-1553 (C=C). $C_{19}H_{17}N_2O_5$ $[M+H]^+$ 353.1131. Found 353.1123.

*N'-(1,4-dioxo-1,4-dihydronaphthalen-2-yl)-3,4,5-trimethoxybenzohydrazide (**14**)* (Figure S2)

This compound was obtained from hydrazide **10**. Orange solid. Yield 55%. mp = 154.2-163.1 ^{1}H NMR (300 MHz, DMSO-d_6) δ 3.73 (s, 3H), 3.84 (s, 6H), 6.17 (s, 1H), 7.26 (s, 1H), 7.82 (m, 1H), 7.82 (m, 1H), 7.95 (dd, *J* = 7.3 Hz; *J* = 1.5 Hz, 1H), 8.0 (dd, *J* = 7.3 Hz; *J* = 1.5 Hz, 1H), 10.45 (s, 1H), 11.69 (br, 1H). ^{13}C NMR (75 MHz, DMSO-d_6) δ 56.5 ($2CH_3$), 60.5 (CH_3), 105.4 (CH), 111.4 (CH), 125.8 (CH), 126.3 (CH), 128.0 (C), 131.0 (C), 132.3 (CH), 133.6 (CH), 134.8 (CH), 140.9 (C), 153.1 (C), 160.0 (C), 165.8 (C), 181.7 (C=O), 185.1 (C=O). FT-IR (KBr, cm^{-1}) $_{max}$ 3445-3512 (NH), 1644-1677 (C=O), 1459-1588 (C=C). $C_{20}H_{18}N_2O_6K$ $[M+K]^+$ 421.0790. Found 421.1602.

*N'-(1,4-dioxo-1,4-dihydronaphthalen-2-yl)-4-nitrobenzohydrazide (**15**)* (Figure S3)

This compound was obtained from hydrazide **11**. Orange solid. Yield 52%. ^{1}H NMR (300 MHz, DMSO-d_6) δ 5.78 (s, 1H), 7.80 (m, 1H), 7.83 (m, 1H), 7.94 (d, *J* = 6.9 Hz, 1H), 8.02 (d, *J* = 6.9 Hz, 1H), 8.16 (d, *J* = 8.7 Hz, 1H), 8.36 (1d, *J* = 8.7 Hz, H), 9.57 (s, 1H), 11.07 (s, 1H). ^{13}C NMR (75 MHz, DMSO-d_6) δ 102.4 (CH), 124.2 (CH), 125.9 (CH), 126.3 (CH), 129.6 (C), 130.9 (CH), 132.9 (CH), 133.2 (C), 135.4 (CH), 138.2 (C), 148.7 (C), 150.0 (C), 164.4 (C), 181.3 (C=O), 182.7 (C=O). FT-IR (KBr, cm^{-1}) v_{max} 3451-3516 (NH), 1644-1782 (C=O), 1459-1592 (C=C). $C_{20}H_{19}N_2O_6$ $[M+H]^+$ 338.0771. Found 338.0762.

*4-bromo-N'-(1,4-dioxo-1,4-dihydronaphthalen-2-yl) benzohydrazide (**16**)* (Figure S4)

This compound was obtained from hydrazide **12**. Brown solid. Yield 55%. ^{1}H NMR (300 MHz, DMSO-d_6) δ 5.71 (s, 1H), 7.77 (m, 1H), 7.77 (m, 1H), 7.87 (m, 1H), 7.95 (d, ^3J = 6 Hz, 1H), 8.02 (d, ^3J = 6 Hz, 1H), 9.50 (s, 1H), 10.82 (s, 1H). ^{13}C NMR (75 MHz, DMSO-d_6) δ 102.2 (CH), 125.9 (CH), 126.3 (CH), 126.4 (CH), 130.0 (C), 130.9 (CH), 132.0 (C), 132.1 (CH), 133.1 (CH), 133.2 (C), 135.4 (C), 148.8 (C), 165.0 (C), 181.4 (C=O), 182.7 (C=O). FT-IR (KBr, cm^{-1}): v_{max} 3451-3516 (NH), 1644-1782 (C=O), 1459-1592 (C=C). $C_{17}H_{12}BrN_2O_6$ $[M+H]^+$ 371.0025. Found 371.0031.

Biological assays

Parasites and cell cultures

Antiparasitic activity experiments were carried out with the Y strain of *Trypanosoma cruzi* (epimastigotes) and promastigotes of *Leishmania amazonensis* (WHOM/BR/75/JOSEFA strain). The forms of epimastigotes were grown in liver infusion tryptose (LIT) medium supplemented with 10% heat-inactivated fetal bovine serum (FBS; Gibco Invitrogen, Grand Island, NY, USA), kept at 28 ° C and maintained by weekly transfers. The promastigote forms of *L. amazonensis* were maintained in culture at 25 ° C with weekly transfers to fresh Warren's medium supplemented with 10% FBS. To evaluate the cytotoxicity of the compounds, LLCMK2 cells (*Macaca mulatta* epithelial kidney cells) were maintained in Dulbecco's modified Eagle medium (DMEM; Gibco Invitrogen), pH 7.4, supplemented with 2 mM L-glutamine, 10% FBS, and 50 $mg.L^{-1}$ gentamicin at 37 ° C in a humidified atmosphere of 5% CO_2.

Antiproliferative Activity against Epimastigote Forms (Trypanosoma cruzi)

Epimastigotes (1×10^6 $parasites.mL^{-1}$) in the exponential growth phase (96 h) were harvested and incubated in the presence of LIT supplemented with 10% FBS added or not to increase concentrations of drug candidates. Subsequently, the incubated organisms at 28 ° C in 96-well flat bottom plates were counted on a Neubauer hemocytometer under light microscopy. IC_{50} (concentration that inhibited

50% parasite growth) was determined by regression analysis of the data.

Antiproliferative activity against promastigote forms (Leishmania amazonensis)

Promastigotes (1 × 10^6 cells.mL^{-1}) in the exponential growth phase (48 h cultures) were inoculated in a 96-well plate in the absence or presence of different concentrations of drug candidates. The activity against promastigote forms was evaluated after 72 h using the XTT method, which consists of incubation of cultures in the presence of a combination of the 2,3-Bis- (2-Methoxy-4-Nitro-5-Sulfophenyl) -2*H*-Tetrazolium-5-Carboxanilide compound (XTT, Sigma) and the electron coupling reagent phenazine methosulfate (PMS, Sigma). After parasite treatment, 100 L of the parasites, 100 µL of the mixture of XTT (0.5 mg.mL^{-1}) and PMS (0.06 mg.mL^{-1}) was added to each well, the plate was incubated for 4 h protected from light at 28 ° C and the absorbance measured at 450 nm in a microplate reader (Bio Tek – Power Wave XS). By comparing the absorbance of the control untreated parasites with those of the treated ones, the inhibitory activity was determined. IC_{50} (concentration that inhibited 50% parasite growth) was determined by regression analysis of the data.

Cytotoxicity Assay

To evaluate the cytotoxicity of the compounds, the MTT assay was applied as previously described (Muñoz et al. 2006). This colorimetric assay is based on the ability of viable mitochondria to convert MTT, a water-soluble salt of tetrazolium salt (3-[4,5-dimethylthiazol-2-yl]-2,5-diphenyltetrazolium bromide), into an insoluble, purple-colored formazan precipitate. LLCMK2 cells were collected from confluent cultures, seeded in 96-well plates, and incubated at 37 ° C in a humid atmosphere of 5% CO2. After 24 h, the medium was replaced with new DMEM that contained concentrations of compounds ranging from 3.7 to 73.6 µM. After 96 h of incubation, cells were washed in PBS and 50 µL of MTT (2 mg.mL^{-1}) was added to each well. The formazan crystals were solubilized in DMSO and absorbance was read at 570 nm on a microplate reader (Bio Tek – Power Wave XS). The concentration that decreased 50% of the absorbance value observed in the control represented the CC_{50} (cytotoxic concentration for 50% of the cells).

Molecular modelling studies

Compounds **13** and **15** were drawn using the program MarvinSketch 16.9.5 (ChemAxon Ltd., Budapest, Hungary). The structure optimization was carried out through PM7 semiempirical method incorporated in the software MOPAC2016 and the definition of charges was made considering a pH of 7.4.

To investigate the potential mechanism of action of these compounds, molecular docking simulations were carried out using cruzain, rhodesain and CPB2.8 as proteins. The 3D structures of cruzain, rhodesain were obtained from the Protein Data Bank (PDB ID: 1AIM and 6EXQ, respectively) (Gillmor et al. 1997, Giroud et al. 2018). Meanwhile, the three-dimensional structure of rCPB2.8 was obtained based on the homology modelling methodology using the Swiss-Model program (Daina et al. 2017). The homology modelling assay followed the procedures described in literature (Lourenço et al. 2023) using papain-like cysteine protease obtained from the Protein Data Bank (PDB ID: 1F2A) as a layout (Brinen et al. 2000) and the primary structure of rCPB2.8 as the target sequence. The molecular docking simulations was carried out using AutoDockVINA software (Trott & Olson 2010). The grid box used for research was large enough to encompass the

target binding site and the crystallographic ligand was deleted before each simulation. Also, the systems of protein and tested compound were subjected to a dock preparation using AutoDockVINA software in which the charges were added through AMBER ff14SB method for standard residues and AM1-BCC method for other residues.

For each protein, the output result of docking simulations with the lowest score value was selected for an optimization of binding mode. The geometry optimizations were made with GROMACS 2018 package and CHARMM force field (Vanommeslaeghe et al. 2010, Zoete et al. 2011). SwissParam Server was used to obtain ligand topology and solvent properties were mimetic based on TIP3P water model (Zoete et al. 2011). A cubic box was built, and its dimensions determined to ensure a space of 1.2 nm between the protein and the walls of the box. The system charges were neutralized with the addition of ions in the physiological condition (0.15μM) and the energy optimization steps were carried out using the steepest descent followed by the conjugate gradient algorithm. The convergent criterion was a maximum of 50 N force on the atoms. Geometry optimization of the solvated system was performed using the steepest descent algorithm, followed by equilibration simulations with nVT and nPT. To perform them, temperature was maintained at 300°K coupling the system to a V-rescale thermostat (0.1 ps) and, using Parinello-Rahman coupling algorithm, the pressure was kept constant at 1 bar. Unrestrained simulations were performed for 1000 ps and the stabilization of all systems were monitored by RMSD and RMSF graphs (Figure S5). After stabilization, the binding free energy was calculated through GROMACS 2018 package considering the short range Columbic and Lennard-Jones interaction energies between compounds and the surroundings. Intermolecular interactions were investigated using the 2D representation provided by LigPlot program (Wallace et al. 1995) and the occupation at the binding site was analyzed using 3D representations using UCSF Chimera.

Acknowledgments

The authors acknowledge Conselho Nacional de Desenvolvimento Científico e Tecnológico - Brazil (CNPq), Coordenação de Aperfeiçoamento de Pessoal de Nível Superior - Brazil (CAPES) - Finance Code 001, Fundação de Apoio ao Desenvolvimento do Ensino, Ciência e Tecnologia – Brazil (FUNDECT – MS) grant n° 266/2022 (SIAFEM 32184 – DPL), FUNDECT-MS (204/2022 – AB). SS and JR would like to acknowledge CNPq (316687/2023-5, 309975/2022-0, 315399/2020-1, 404172/2023-7, and 405655/2023-1). The authors declare that the research was conducted in the absence of commercial or financial relationships that could be construed as a potential conflict of interest.

REFERENCES

ABRAS A, BALLART C, FERNÁNDEZ-ARÉVALO A, PINAZO M-J, GASCÓN J, MUÑOZ C & GÁLLEGO M. 2022. Worldwide Control and Management of Chagas Disease in a New Era of Globalization: A Close Look at Congenital Trypanosoma cruzi Infection. Clin Microbiol Rev 35: e00152-21.

BHAL SK. 2007. Advanced Chemistry Development (ACD/LABS). Log P—Making Sense of the Value; Advanced Chemistry Development: Toronto, ON, Canada.

BOTTESELLE GV ET AL. 2021. Catalytic antioxidant activity of bis-aniline-derived diselenides as GPx mimics. Molecules 26: 4446.

BOUHADIR K, ATALLAH H, MEZHER R, FATFAT M, GALI-MUHTASIB G & ELARIDI J. 2017. Synthesis and biological assessment of novel acylhydrazone derivatives of 2-methyl-1,4-naphthoquinone. Org Comm 10: 259-272.

BRINEN LS, HANSELL E, CHENG J, ROUSH WR, MCKERROW JH & FLETTERICK RJ. 2000. A Target within the Target: Probing Cruzain's P1' Site to Define Structural Determinants for the Chagas' Disease Protease. Structure 8: 831-840.

BROWN N. 2012. Bioisosterism in Medicinal Chemistry, p 1-14, Bioisosteres in Medicinal Chemistry, vol 54. Wiley-VCH, United Kingdom.

BURKNER GT ET AL. 2023. Selenylated Imidazo[1,2-a] pyridine Induces Cell Senescence and Oxidative Stress in Chronic Myeloid Leukemia Cells. Molecules 28: 893.

CAFFREY CR, SCHANZ M, NKEMGU-NJINKENG J, BRUSH M, HANSELL E, COHEN FE, FLAHERTY TM, MCKERROW JH & STEVERDING D. 2002. Screening of acyl hydrazide proteinase inhibitors for antiparasitic activity against Trypanosoma brucei. Int J Antimicrob Agents 19: 227-231.

CARDOSO MFC, FOREZI LSM, CAVALCANTE VGS, JULIANI CSR, RESENDE JALC, ROCHA DRD, SILVA FCD & FERREIRA VF. 2017. Synthesis of new xanthenes based on Lawsone and Coumarin via a tandem three-component reaction. J Braz Chem Soc 28: 1926-1936.

DA SILVA AO, LOPES RS, DE LIMA RV, TOZATTI CSS, MARQUES MR, DE ALBUQUERQUE S, BEATRIZ A & DE LIMA DP. 2013. Synthesis and biological activity against Trypanosoma cruzi of substituted 1,4-naphthoquinones. Eur J Med Chem 60: 51-56.

DAINA A, MICHIELIN O & ZOETE V. 2017. SwissADME: A Free Web Tool to Evaluate Pharmacokinetics, Drug-Likeness and Medicinal Chemistry Friendliness of Small Molecules. Sci Rep 7: 42717.

DANTAS E ET AL. 2017. Characterization and trypanocidal activity of a novel pyranaphthoquinone. Molecules 22: 1631.

DE CASTRO SL, EMERY FS & DA SILVA JUNIOR EN. 2013. Synthesis of quinoidal molecules: Strategies towards bioactive compounds with an emphasis on lapachones. Eur J Med Chem 69: 678-700.

DONG J, DU Y & ZHOU L. 2023. Research progress of CRISPR/Cas systems in nucleic acid detection of infectious diseases. iLABMED 1: 58-74.

DOS SANTOS DC ET AL. 2021. Apoptosis oxidative damage-mediated and antiproliferative effect of selenylated imidazo[1,2-a]pyridines on hepatocellular carcinoma HepG2 cells and in vivo. J. Biochem Mol Toxicol 35: E22663.

DOS SANTOS DC, RAFIQUE J, SABA S, GRINEVICIUS VMAS, FILHO DW, ZAMONER A, BRAGA AL, PEDROSA RC & OURUIQUE F. 2022. IP-Se-06, a Selenylated Imidazo[1,2-a]pyridine, Modulates Intracellular Redox State and Causes Akt/mTOR/HIF-1α and MAPK Signaling Inhibition, Promoting Antiproliferative Effect and Apoptosis in Glioblastoma Cells. Oxid Med Cell Longev 2022: Article ID 3710449.

DUDLEY KH, MILLER HW, SCHNEIDER PW & MCKEE RL. 1969. Potential naphthoquinone antimalarials. 2-Acylhydrazino-1,4-naphthoquinones and related compounds. J Org Chem 34: 2750-2755.

FRAGA CAM. 2009. Drug hybridisation strategies: before or after lead identification? Expert Opin Drug Discov 4: 605-609.

FRANCO MS, SABA S, RAFIQUE J & BRAGA AL. 2021. KIO4-mediated Selective Hydroxymethylation/Methylenation of Imidazo-Heteroarenes: A Greener Approach. Angew Chem Int Ed 60: 18454-18460.

FERSHTAT LL & MAKHOVA NN. 2017. Molecular Hybridisation Tools in the Development of Furoxan-Based NO-Donor Prodrugs. ChemMedChem 12: 622-638.

GILBERT IH. 2013. Drug Discovery for Neglected Diseases: Molecular Target-Based and Phenotypic Approaches. J Med Chem 56: 7719-7726.

GILLMOR SA, CRAIK CS & FLETTERICK RJ. 1997. Structural determinants of specificity in the cysteine protease cruzain. Protein Sci 6: 1603-1611.

GIROUD M ET AL. 2018. Repurposing a Library of Human Cathepsin L Ligands: Identification of Macrocyclic Lactams as Potent Rhodesain and Trypanosoma brucei Inhibitors. J Med Chem 61: 3350-3369.

GUIMARÃES TT ET AL. 2013. Potent naphthoquinones against antimony-sensitive and -resistant Leishmania parasites: Synthesis of novel α- and nor-α-lapachone-based 1,2,3-triazoles by copper-catalyzed azide–alkyne cycloaddition. Eur J Med Chem 63: 523-530.

HERWALDT BB. 1999. Leishmaniasis. Lancet 354: 1191-1199.

HU B, YAN W, JIANG P, JIANG L, YUAN X, LIN J, JIAO Y & JIN Y. 2023. Switchable synthesis of natural-product-like lawsones and indenopyrazoles through regioselective ring-expansion of indantrione. Commun Chem 6: 17.

JORGE J ET AL. 2023 Recent Advances on the Antimicrobial Activities of Schiff Bases and their Metal Complexes: An Updated Overview. Curr Med Chem DOI: 10.2174/0929867330666230224092830.

KAVITHA RANI PR, FERNANDEZ A, GEORGE A, REMADEVI VK, SUDARSANAKUMAR MR, LAILA SP & ARIF M. 2015. Synthesis, spectral characterization, molecular structure and pharmacological studies of N'-(1, 4-naphtho-quinone-2yl) isonicotinohydrazide. Spectrochim Acta A Mol Biomol Spectrosc 135: 1156-1161.

KUMAR P, KADYAN K, DUHAN M, SINDHU J, SINGH V & SAHARAN BS. 2017. Design, synthesis, conformational and molecular docking study of some novel acyl hydrazone based molecular hybrids as antimalarial and antimicrobial agents. Chem Cent J 11: 115.

LANGDON SR, ERTL P & BROWN N. 2010. Bioisosteric Replacement and Scaffold Hopping in Lead Generation and Optimization. Mol Inform 29: 366-385.

LAZAR C, KLUCZYK A, KIYOTA T & KONISHI Y. 2004. Drug Evolution Concept in Drug Design: 1. Hybridisation Method. J Med Chem 47: 6973-6982.

LIPINSKI CA, LOMBARDO F, DOMINY BW & FEENEY PJ. 1997. Experimental and Computational Approaches to Estimate Solubility and Permeability in Drug Discovery and Development Settings. Adv Drug Deliv Rev 23: 3-25.

LOURENÇO EMG ET AL. 2023. Flavonoid Derivatives as New Potent Inhibitors of Cysteine Proteases: An Important Step toward the Design of New Compounds for the Treatment of Leishmaniasis. Microorganisms 11: 225.

MARTIN YC, KOFRON JL & TRAPHAGEN LM. 2002. Do Structurally Similar Molecules Have Similar Biological Activity? J Med Chem 45: 4350-4358.

MOLFETTA FA, BRUNI AT, HONÓRIO KM & DA SILVA ABF. 2005. A structure–activity relationship study of quinone compounds with trypanocidal activity. Eur J Med Chem 40: 329-338.

MORAES COA ET AL. 2023. Urea Hydrogen Peroxide and Ethyl Lactate, an Eco-Friendly Combo System in the Direct C(sp^2)–H Bond Selenylation of Imidazo[2,1-*b*]thiazole and Related Structures. Acs Omega 8: 39535-39545.

MUÑOZ DLP, CARDONA D, CARDONA A, CARRILLO LM, QUIÑONES W, ECHEVERRI F, VÉLEZ ID & ROBLEDO SM. 2006. Effect of hydrazones on intracellular amastigotes of Leishmania panamensis and a parasite cysteine protease. Vitae 13: 05-12.

NASIM F & QURESHI IA. 2023. Aminoacyl tRNA Synthetases: Implications of Structural Biology in Drug Development against Trypanosomatid Parasites. ACS Omega 8: 14884-148899.

NAUJORKS AADS, DA SILVA AO, LOPES RDS, DE ALBUQUERQUE S, BEATRIZ A, MARQUES MR & DE LIMA DP. 2015. Novel naphthoquinone derivatives and evaluation of their trypanocidal and leishmanicidal activities. Org Biomol Chem 13: 428-437.

NAVARRO-TOVAR G, VEGA-RODRIGUEZ S, LEYVA E, LOREDO-CARRILLO S, DE LOERA D & LOPEZ-LOPEZ LI. 2023. The Relevance and Insights on 1,4-Naphthoquinones as Antimicrobial and Antitumoral Molecules: A Systematic Review. Pharmaceuticals 16: 496.

NICOLÁS-HERNÁNDEZ DSA, HERNÁNDEZ-ÁLVAREZ E, BETHENCOURT-ESTRELLA CJ, LÓPEZ-ARENCIBIA A, SIFAOUI I, BAZZOCCHI IL, LORENZO-MORALES J, JIMÉNEZ IA & PIÑERO JE. 2023. Multi-target withaferin-A analogues as promising anti-kinetoplastid agents through the programmed cell death. Biomed Pharmacother 164: 114879.

OLIVIER M, GREGORY DJ & FORGET G. 2005. Subversion Mechanisms by which Leishmania Parasites Can Escape the Host Immune Response: A Signaling Point of View Clin Microbiol Rev 18:293-305.

PEDROSO GJ ET AL. 2023. Selenylated indoles: synthesis, effects on lipid membrane properties and DNA cleavage. New J Chem 47: 2719-2726.

RAFIQUE J ET AL. 2020. Selenylated-oxadiazoles as promising DNA intercalators: Synthesis, electronic structure, DNA interaction and cleavage. Dyes Pigm 180: 108519.

RANI R, SETHI K, KUMAR S, VARMA RS & KUMAR R. 2022. Natural naphthoquinones and their derivatives as potential drug molecules against trypanosome parasites. Chem Biol Drug Des 100: 786-817.

REBELLO KM ET AL. 2010. Leishmania (Viannia) braziliensis: Influence of successive in vitro cultivation on the expression of promastigote proteinases. Exp Parasitol 126: 570-576.

REDDY MRD, PRASAD ARG, SPOORTHY YN & RAVINDRANATH LRKR. 2013. Synthesis, Characterization and Antimicrobial Activity of Certain Novel Aryl Hydrazone Pyrazoline-5-Ones Containing Thiazole Moiety. Adv Pharm Bull 3: 153-159.

RODRIGUES DA, FERREIRA-SILVA GÀ, FERREIRA ACS, FERNANDES RA, KWEE JK, SANT'ANNA CMR, IONTA M & FRAGA CAM. 2016. Design, Synthesis, and Pharmacological Evaluation of Novel N-Acylhydrazone Derivatives as Potent Histone Deacetylase 6/8 Dual Inhibitors. J Med Chem 59: 655-670.

RODRIGUES JHDS, UEDA-NAKAMURA T, CORRÊA AG, SANGI DP & NAKAMURA CV. 2014. A Quinoxaline Derivative as a Potent Chemotherapeutic Agent, Alone or in Combination with Benznidazole, against Trypanosoma cruzi. PLoS ONE 9: e85706.

RYCKER MD, WYLLIE S, HORN D, READ KD & GILBER IH. 2023. Anti-trypanosomatid drug discovery: progress and challenges. Nat Rev Microbiol 21:35-50.

SALAS C, TAPIA RA, CIUDAD K, ARMSTRONG V, ORELLANA M, KEMMERLING U, FERREIRA J, MAYA JD & MORELLO A. 2008. Trypanosoma cruzi: Activities of lapachol and α- and β-lapachone derivatives against epimastigote and trypomastigote forms. Bioorg Med Chem 16: 668-674.

SANDER T. 2001. OSIRIS Property Explorer; Organic Chemistry Portal: Basel, Switzerland.

SCHEIDE MR ET AL. 2020. Borophosphate glass as an active media for CuO nanoparticle growth: An efficient catalyst for selenylation of oxadiazoles and application in redox reactions. Sci Rep 10: 15233.

SCHENONE M, DANČÍK V, WAGNER BK & CLEMONS PA. 2013. Target identification and mechanism of action in chemical biology and drug discovery. Nat Chem Biol 9: 232-240.

SILVA-JARDIM I, THIEMANN OH & ANIBAL FF. 2014. Leishmaniasis and Chagas disease chemotherapy: a critical review. J Braz Chem Soc 25: 1810-1823.

SILVA LR, GUIMARAES AS, NASCIMENTO J, NASCIMENTO IJS, SILVA EB, MCKERROW JH, CARDOSO SH & SILVA-JÚNIOR EJ. 2021. Computer-aided design of 1,4-naphthoquinone-based inhibitors targeting cruzain and rhodesain cysteine proteases. Bioorg Med Chem 41: 116213.

SINGH R, KASHIF M, SRIVASTAVA P & MANNA PP. 2023. Recent Advances in Chemotherapeutics for Leishmaniasis: Importance of the Cellular Biochemistry of the Parasite and Its Molecular Interaction with the Host. Pathogens 12: 706.

STUMPFE D, HU H & BAJORATH J. 2019. Evolving Concept of Activity Cliffs. ACS Omega 4: 14360-14368.

TROTT O & OLSON AJ. 2010. AutoDock Vina: Improving the speed and accuracy of docking with a new scoring function, efficient optimization, and multithreading. Comput Chem 31: 455-461.

VELOSO IC ET AL. 2021. A selanylimidazopyridine (3-SePh-IP) reverses the prodepressant- and anxiogenic-like effects of a high-fat/high-fructose diet in mice. J Pharm Pharmacol 73: 673-681.

VENKATESAN G, AB RAHMAN WSW, SHAHIDAN WNS, IBERAHIM S & BESARI@HASHIM ABM. 2023. Plasma-derived exosomal miRNA as potential biomarker for diagnosis and prognosis of vector-borne diseases: A review. Front Microbiol 14: 1097173.

VANOMMESLAEGHE K ET AL. 2010. CHARMM General Force Field: A Force Field for Drug-like Molecules Compatible with the CHARMM All-atom Additive Biological Force Fields. J Comput Chem 31: 671-690.

VÁSCONEZ-GONZÁLEZ J, IZQUIERDO-CONDOY JS, FERNANDEZ-NARANJO R, GAMEZ-RIVERA E, TELLO-DE-LA-TORRE A, GUERRERO-CASTILLO GS, RUIZ-SOSA C & ORTIZ-PRADO E. 2023. Severe Chagas disease in Ecuador: a countrywide geodemographic epidemiological analysis from 2011 to 202. Front Public Health 11: 1172955.

VERDAN M, TAVEIRA I, LIMA F, ABREU F & NICO D. 2023. Drugs and nanoformulations for the management of Leishmania infection: a patent and literature review (2015-2022). Expert Opin Ther Pat 33: 137-150.

VIEGAS-JUNIOR C, DANUELLO A, BOLZANI VS, BARREIRO EJ & FRAGA CAM. 2007. Molecular hybridisation: A useful tool in the design of new drug prototypes. Curr Med Chem 14: 1829-1852.

VITOR N, MEZA A, GOMES RS, RAFIQUE J, DE LIMA DP & BEATRIZ A. 2021. Straightforward synthesis of cytosporone analogs AMS35AA and AMS35BB. An Acad Bras Cienc 93: e20201347.

WALLACE AC, LASKOWSKI RA & THORNTON JM. 1995. LIGPLOT: a program to generate schematic diagrams of protein-ligand interactions. Protein Eng 8: 127-134.

WANG Z, XIONG Y, PENG Y, ZHANG X, LI S, PENG Y, PENG X, ZHUO L & JIANG W. 2023. Natural product evodiamine-inspired medicinal chemistry: Anticancer activity, structural optimization and structure-activity relationship. Eur J Med Chem 247: 115031.

WARUSAVITHANA S, ATTA H, OSMAN M & HUTIN Y. 2022. Review of the neglected tropical diseases programme implementation during 2012– 2019 in the WHO-Eastern Mediterranean Region. PLOS Negl Trop Dis 16: e0010665.

WHO. 2017. Chagas disease (American trypanosomiasis). http://www.who.int/chagas/en/. Accessed 31st March 2023.

WHO. 2020. Neglected tropical diseases. Draft road map for neglected tropical diseases 2021–2030.

ZOETE V, CUENDET MA, GROSDIDIER A & MICHIELIN O. 2011. SwissParam: A Fast Force Field Generation Tool for Small Organic Molecules. J Comput Chem 32: 2359-2368.

SUPPLEMENTARY MATERIAL

Figure S1-S6.

How to cite

CEZAR RD, SILVA AO, LOPES RS, NAKAMURA CV, RODRIGUES JHS, LOURENÇO EMG, SABA S, BEATRIZ A, RAFIQUE J & LIMA DP. 2024. Design, synthesis and identification of novel molecular hybrids based on naphthoquinone aromatic hydrazides as potential trypanocide and leishmanicidal agents. An Acad Bras Cienc 96: e20230375. DOI 10.1590/0001-3765202420230375.

Manuscript received no April 5, 2023;
accepted for publication on July 6, 2023

ROSANE D. CEZAR[1]
https://orcid.org/0000-0003-4350-7939

ADRIANO O. DA SILVA[2]
https://orcid.org/0000-0001-6608-7522

ROSÂNGELA S. LOPES[1]
https://orcid.org/0000-0003-0549-0697

CELSO V. NAKAMURA[3]
https://orcid.org/0000-0002-9911-7369

JEAN HENRIQUE S. RODRIGUES[3]
https://orcid.org/0000-0003-2902-4578

ESTELA MARIANA G. LOURENÇO[1]
https://orcid.org/0000-0003-2708-4526

SUMBAL SABA[4]
https://orcid.org/0000-0002-6134-7249

ADILSON BEATRIZ[1]
https://orcid.org/0000-0001-6864-6092

JAMAL RAFIQUE[1]
https://orcid.org/0000-0002-2336-040X

DÊNIS P. DE LIMA[1]
https://orcid.org/0000-0002-6023-4867

[1]Universidade Federal do Mato Grosso do Sul – UFMS, Instituto de Química, Av. Senador Filinto Müller, 1555, Cidade Universitária, 79074-460 Campo Grande, MS, Brazil

[2]Universidade Federal de Mato Grosso – UFMT, Departamento de Química, Av. Fernando Corrêa da Costa, 2367, Boa Esperança, 78060-900 Cuiabá, MT, Brazil

[3]Universidade Estadual de Maringá – UEM, Laboratório de Inovação Tecnológica no Desenvolvimento de Fármacos e Cosméticos, Av. Colombo, 5790, Jd. Universitário, 87020-900 Maringá, PR, Brazil

[4]Universidade Federal de Goiás – UFG, LabSO, Instituto de Química, Avenida Esperança s/n, Câmpus Samambaia, 74690-900 Goiânia, GO, Brazil

Correspondence to: **Dênis Pires de Lima / Jamal Rafique**
E-mail: denis.lima@ufms.br / jamal.chm@gmail.com, jamal.rafique@ufms.br

Author contributions

Rosane Dias Cezar: data curation, investigation, methodology, writing – original draft. Adriano O. da Silva: data curation, methodology. Rosângela da S. Lopes: data curation, methodology. Celso V. Nakamura: biological evulation, investigation.Jean H. da Silva Rodrigues: biological evulation, investigation.Estela M. Guimarães: molecular modeling studies, investigation. Sumbal Saba: data curation, formal analysis, visualization. Adilson Beatriz: formal analysis, visualization. Jamal Rafique: conceptualization, funding acquisition, supervision, formal analysis, writing – original draft and review & editing. Dênis Pires de Lima: funding acquisition, supervision, writing – review & editing.